



A paper-based assay for detecting hypervirulent *Klebsiella pneumoniae* using CRISPR-Cas13a system

Gargi Bhattacharjee^a, Nisarg Gohil^a, Khushal Khambhati^a, Devarshi Gajjar^b, Ali Abusharha^c, Vijai Singh^{a,*}

^a Department of Biosciences, School of Science, Indrashil University, Rajpur, Mehsana 382715, Gujarat, India

^b Department of Microbiology and Biotechnology Centre, Faculty of Science, The Maharaja Sayajirao University of Baroda, Vadodara 390002, Gujarat, India

^c Optometry Department, Applied Medical Sciences College, King Saud University, P.O. Box 145111, Riyadh, Saudi Arabia

ARTICLE INFO

Keywords:

Klebsiella pneumoniae
CRISPR-Cas13a
Hypervirulent
Diagnostics
Multidrug resistance

ABSTRACT

Klebsiella pneumoniae, a prevalent healthcare-associated pathogen, poses a significant challenge to diagnosis and treatment due to its virulence and antimicrobial resistance. The demand for more efficient, precise and accessible diagnostic methods is imperative, as current approaches are labor-intensive and resource-dependent. In this study, a CRISPR (Clustered Regularly Interspaced Short Palindromic Repeats)-based diagnostic tool for rapid detection of hypervirulent *K. pneumoniae* infections was proposed. We integrated recombinase polymerase amplification (RPA) coupled with a lateral flow assay and Cas13a (CRISPR associated protein 13a) to target the housekeeping *rpoB* gene for species-specific detection and the capsular polysaccharide regulating gene *rmpA* for identification of hypervirulent strains of *K. pneumoniae*. Tested on 18 *K. pneumoniae* strains, the devised tool successfully detected hypervirulent strains *K. pneumoniae* M59 and *K. pneumoniae* KP109 showing presence of *rmpA*. This study allows to develop an instrument-free platform for routine diagnosis of *K. pneumoniae* from serum, urine, and saliva samples that would empower healthcare personnel to facilitate proper and timely treatment of infections caused by the *K. pneumoniae*.

1. Introduction

Rapid, convenient and efficient diagnosis of infectious diseases are vital for ensuring clinical care, directing infection control and public health initiatives to restrict disease transmission in highly equipped medical centers as well as remote healthcare settings with limited resources. An ideal diagnostic procedure could be the one which is rapid, affordable, error-free, and enables point-of-care (POC) operation without the necessity of a technically trained person, expensive instrumentation, or power supply. A test that endows these features could aid in the early detection of highly virulent pathogens, conscious isolation to prevent disease spread, and facilitate prompt medical attention and timely cure [1].

The menace of antimicrobial resistance is a call for urgent attention towards global health, as an effect of which, in 2019 alone, nearly 5 million people worldwide fell prone to the factor directly attributable to drug resistance and lost their lives, claims a study published in The Lancet [2]. The Centers for Disease Control and Prevention (CDC)

broadly categorizes pathogens as urgent, serious, and concerning groups based on the threats they possess [3]. It is asserted by the CDC that committed prevention and disease control initiatives could cut down fatalities arising from antibiotic-resistant illnesses. A significant portion of progress made in combating antimicrobial resistance was lost, mostly as a consequence of the pandemic, according to the CDC's 2022 special report detailing COVID-19's effects on antibiotic resistance [4]. The pandemic challenged health departments, healthcare centers, and the general population frighteningly near breaking point and made it immensely difficult to sustain the progress made against the antimicrobial resistance.

Opportunistic bacterial pathogens that are generally thought of as commensals but prey on weakened immune systems and disturbed microbiomes of hospitalised patients to cause maladies are particularly vicious [5–7]. Of the pool of pathogens responsible for causing hospital-acquired infections (HAIs), especially concerning are the Gram-negative bacteria including *Klebsiella pneumoniae*, which has acquired resistance to ampicillin and exhibits multidrug resistance (MDR) to several other

* Corresponding author.

E-mail addresses: vijaisingh15@gmail.com, vijai.singh@indrashiluniversity.edu.in (V. Singh).

medications [8]. Antimicrobial-resistant (AMR) *K. pneumoniae* was recognized by CDC as an organism demanding immediate attention and placed under the urgent category [3]. This leaves very few choices for antibiotic therapy since *K. pneumoniae* readily acquires virulence-causing and AMR genes through the transmission of mobile genetic elements, which confers resistance to third-generation cephalosporins and carbapenems [9]. *K. pneumoniae* stands among the leading pathogens causing HAIs around the world, causing pneumonia, urinary tract infections, wound infections and surgical site sepsis [6,10]. Investigations also demonstrate that this bacterium played a significant role in infant sepsis in Africa and Asia, and is an obvious opportunist, which frequently colonises the human gut, nasopharynx, and skin [11,12]. The carbapenem-resistant *K. pneumoniae* is particularly vicious as it can effortlessly acquire virulent genes through the transmission of mobile genetic elements. Currently, *K. pneumoniae* is mostly detected using phenotype-based approaches of identification, such as biochemical markers [13] or bacterial recognition systems [14]. Many times, matrix-assisted laser desorption/ionization-time of flight mass spectrometry (MALDI-TOF MS) is also used to detect *K. pneumoniae* [15]. However, a limiting factor of the aforementioned techniques is that these techniques are culture-based and therefore it requires longer diagnosis time, leading to delay.

With nucleic acid-based detection, it is easier to diagnose pathogens at an early stage and prevent the spread of infections. Polymerase chain reactions (PCRs)-based molecular diagnostic techniques devised to detect *K. pneumoniae* that have presented propitious outcomes, but this technology necessitates the requirement of expensive instrumentation, skilled professionals and long reaction time. Some key isothermal amplification technologies presently in use include recombinase polymerase amplification (RPA), strand displacement amplification (SDA), rolling circle amplification (RCA), helicase-dependent isothermal DNA amplification (HDA), nucleic acid sequence-based amplification (NASBA) and loop-mediated isothermal amplification (LAMP). RPA is relatively the simplest of all these technologies and therefore it is adopted in applications requiring rapid nucleic acid amplification [16].

Currently, clustered regularly interspaced short palindromic repeats (CRISPR) and the associated proteins (Cas) are the most intensively genome editing tools of the modern era [17–20]. Persistent research in this area has unearthed several different CRISPR toolboxes and since then many CRISPR-based technologies have materialized [21–24]. Recent years have witnessed the advancements of several CRISPR-Cas variants based detection platforms that have shown great sensitivity and ultra-specificity. Such tools make use of either Cas9 enzyme which determines the presence of pathogens by specifically recognizing, binding and cleaving the target nucleic acid sequence [25], or other Cas nucleases such as Cas12 and Cas13 which rely on pathogen detection by virtue of their collateral cleavage ability [26,27]. The ability of this technology to specifically target virulence and drug-resistant genes both chromosomally encoded as well as plasmid-borne, without impacting healthy bacterial populations makes it a potential antimicrobial arsenal. Aside from its use in AMR therapy, CRISPR-Cas system when integrated with other approaches could endow diagnostic tools with on-site applications giving instrument-free readouts. CRISPR systems when combined with the RPA approach of isothermal amplification method for nucleic acid detection could harness the rapidity and convenience of RPA, leading to detection and intervention at the early stages of infection onset [28].

In this work, we employed a simple instrument-free CRISPR detection platform with RPA to first demonstrate the detection of *Klebsiella* spp. by detecting the species-specific housekeeping *rpoB* gene of *K. pneumoniae*. We then proceeded to detect the hypervirulent strains of *K. pneumoniae* amongst the clinical strains of the organism by targeting a capsular polysaccharide regulating *rmpA* gene. The limit of detection of the present method was determined. Importantly, the protein purification steps are relatively simple and do not demand any tedious purification procedures, and therefore it can be executed with minimal to no

instrumentation support except for a centrifuge.

2. Materials and methods

2.1. Strains and plasmids

In this study, 18 strains of *K. pneumoniae* and six other strains (*Escherichia coli*, *Staphylococcus aureus*, *Pseudomonas aeruginosa*, *Serratia marcescens*, *Chromobacterium violaceum* and *Bacillus subtilis*) belonging to different genera were used. Fifteen out of the eighteen clinical strains of *K. pneumoniae* were provided by The Maharaja Sayajirao University of Baroda, Vadodara, India. The genomic DNA of all the strains used in the study were extracted manually using a simple phenol–chloroform extraction method demonstrated by Cheng and Jiang [29]. Strains *E. coli* DH5 α and *E. coli* BL21(DE3) were used for cloning experiments and as expression host of the recombinant vectors, respectively. All the bacterial strains were grown and maintained in Luria Bertani (LB) medium (HiMedia, India) at 37 °C. Plasmid pC019 harbouring the *LwaCas13a* gene of the *Leptotrichia wadei* origin was kindly gifted by Prof. Feng Zhang and procured from Addgene repository (Plasmid #91909). The pET28a expression vector was used for the construction of Cas13a plasmid.

2.2. Cloning, expression and purification of recombinant *LwaCas13a*

The purified Cas13 protein is among the key components of the *in vitro* testing of the diagnostic assay. Hence, the *LwaCas13a* gene (3.4 kb) was amplified from plasmid pC019 using Cas13a_pET28aF and Cas13a_pET28aR primers (Table 1) that was digested by *SacI* and *HindIII* and ligated to *SacI*/*HindIII*-digested pET28a followed by its transformation into chemical competent *E. coli* DH5 α . Clones were screened and sequence was verified. Confirmed clone was named as SHER10. SHER10 was transformed into chemically competent *E. coli* BL21(DE3) pLysS cells using the heat shock method and gene expression was induced at the mid-log phase in the cells of *E. coli* BL21(DE3) pLysS with 0.75 mM isopropyl β -D-1-thiogalactopyranoside (IPTG). Following 16 h incubation, cells expressing hexa-histidine-tagged Cas13a protein were centrifuged and stored at -80 °C until further use.

The Cas13a protein was purified through means of Ni-NTA affinity chromatography by using Ni-NTA Spin Kit (QIAGEN, Germany) according to the manufacturer's protocol with minor modifications. Briefly, the frozen cell pellet was resuspended in lysis buffer (50 mM NaH₂PO₄, 300 mM NaCl, 10 mM imidazole, pH 8.0), 3U Benzonase® per culture volume (Thermo Scientific, USA) and 100 μ L lysozyme stock solution (10 mg ml⁻¹) (Thermo Scientific, USA). All protein purification steps were carried out on ice. The suspension was incubated at 37 °C for 30 min. The cells were then disrupted by a 7–10 cycles of pulse sonication and the lysed suspension was centrifuged to separate the clear lysate from the cell debris. In case of unavailability of a sonicator, this step can be skipped, just the protein output would be comparatively less. The supernatant was then applied onto an equilibrated Ni-NTA column and centrifuged at 100 g until the entire applied volume of supernatant passed through. The column was washed thrice, once with 0.5–1 volume of wash buffer NPI–20 (50 mM NaH₂PO₄, 300 mM NaCl, 20 mM imidazole, pH 8.0), followed by 0.5–1 volume of wash buffer NPI–60 (50 mM NaH₂PO₄, 300 mM NaCl, 60 mM imidazole, pH 8.0), and at once with 0.5–1 volume of wash buffer NPI–60 (50 mM NaH₂PO₄, 300 mM NaCl, 60 mM imidazole, pH 8.0) to remove most of the non-specifically bound proteins. The protein was eluted using elution buffer NPI–500 (50 mM NaH₂PO₄, 300 mM NaCl, 500 mM imidazole) in two subsequent elution steps.

To purify the protein further, after chromatography, the Cas13a protein fractions were combined and dialyzed using a Slide-a-Lyzer dialysis cassette (ThermoScientific, USA) against dialysis buffer (50 mM Tris HCl, 600 mM NaCl, 2 mM DTT, pH of 8.0) for 24 h at 4 °C with constant stirring over a magnetic stirrer. The dialyzed elute was buffer

Table 1
A list of all primers and probes used in this study.

Primer/probe	Sequence (5'–3')	Nucleotides	Purpose	Reference
Cas13a_pET28aF	AATGAGCTCATGAAAGTAGCACCAGGTCGACGG	32	To amplify Cas13a gene	This study
Cas13a_pET28aR	ATAAAGCTTTTCCAGGCGCTGTACTCGAAGATC	34		
rmpA-PCR/F	ACTGGGCTACCTCTGCTTCA	20	To ensure presence of <i>rmpA</i> in the <i>K. pneumoniae</i> strains used in this study	[33]
rmpA-PCR/R	CTTGCATGAGGCATCTTTCA	20		
rpob-RPA/F	GAAATTAATACGACTACTATAGGTCAAAAGACATTAAAGAAACAAGAAGTCTACA	55	RPA primer set for pre-amplification of <i>rpob</i> in <i>K. pneumoniae</i>	This study
rpob-RPA/R	GATGATACGTGGGTTTACAGAACCTTAC	29		
rmpA-RPA/F1	GAAATTAATACGACTACTATAGGTTAATAAATCAATAGCAATTAAGCACAAAAGAAAC	60	RPA primer sets for pre-amplification of <i>rmpA</i> in <i>K. pneumoniae</i>	
rmpA-RPA/F2	GAAATTAATACGACTACTATAGGTTAATAAATCAATAGCAATTAAGCACAAAAGAAAC	60		
rmpA-RPA/R1	GAAATTAATACGACTACTATAGGTTAATAAATCAATAGCAATTAAGCACAAAAGAAAC	35		
rmpA-RPA/R2	CTATCATATTTATTGATCCCTTAACATTTTGTGA	35		
rpob crRNA	TATCAATTAATGATCCCTTAACATTTTGTACC	89	crRNA targeting <i>K. pneumoniae</i> <i>rpob</i>	
rmpA crRNA	GCTCCACAAATAGCAAAGAGTCGAGTGTGTTTAAAGTCCCTTCCGTTTGGGTTAGTCTAAATCCCTATAGTGTGTTAAATTTTC	89	crRNA targeting <i>K. pneumoniae</i> <i>rmpA</i>	
T7 primer	CAACTGTCCTCTAAAATAAAGTCCCTGTTTGTAGTCCCTTCCGTTTGGGTTAGTCTAAATCCCTATAGTGTGTTAAATTTTC	89	T7 promoter annealing sequence for IVT	[30]
LFA-RNA reporter	GAAATTAATACGACTACTATAGG /56-FAM/7UrUrUrUrU/3Bio/	25	ssRNA reporter molecule for <i>trans</i> -cleavage by LwaCas13a	

Bio biotin, FAM fluorescein, IVT *in vitro* transcription, ssRNA single-stranded RNA.

exchanged to storage buffer (50 mM Tris HCl, 600 mM NaCl, 2 mM DTT, 15 % v/v glycerol, pH of 8.0) and stored in aliquots at -80°C until further use. Protein concentrations were measured spectrophotometrically at 280 nm wavelength using NanoDrop (Thermo Scientific, USA).

2.3. Designing of RPA primers, probes and crRNA

Klebsiella-specific *rmpA* gene was retrieved from GenBank (GenBank no. AY059958.1) in the FASTA format, and the conserved region was chosen to design RPA primers using NCBI Primer-Blast server (<https://www.ncbi.nlm.nih.gov/tools/primer-blast/>). Parameters used to design primers were mostly default with the exception of amplicon size in between 100–120 bp, melting temperature between $54\text{--}67^{\circ}\text{C}$ and the primer size between 25–35 nt in length. T7 RNA polymerase promoter sequence was appended to the 5' end of the forward RPA primers to allow T7 transcription. Primers and oligonucleotides were ordered from Eurofins Scientific (Bangalore, India) (Table 1).

The pre-crRNAs were initially synthesized as a single-stranded DNA oligonucleotide template containing a spacer sequence joined with a 5' direct repeat sequence to form a complete crRNA and a T7 RNA polymerase promoter sequence upstream of the crRNA sequence for the T7 transcription to take place. The entire sequence was ordered as the DNA reverse complement template. Multiple Primer Analyzer tool (ThermoFisher Scientific) was used to ensure that both RPA primers and crRNAs with probabilities to form self-dimers or cross-primer dimers were not taken through to production.

2.4. Preparation, *in vitro* transcription and purification of crRNA

The crRNAs were created in accordance with the recommendations of Kellner et al. [30]. The crRNA template was flanked by a 5' T7 RNA polymerase promoter binding sequence to allow transcription to take place. The crRNAs were transcribed *in vitro* using methods described in earlier studies [30,31]. Synthetic single-stranded DNA templates (Integrated DNA Technologies, USA) synthesized as reverse complement of the desired crRNA repeat construct were annealed to an oligonucleotide sequence corresponding to the T7 promoter primer sequence (Table 1).

To proceed with *in vitro* transcription (IVT), 1 μL crRNA template (100 μM) at a final concentration of 10 μM was mixed with 1 μL 10 \times standard Taq buffer (Thermo Scientific, USA) and 1 μL T7 IVT primer (100 μM) and the final volume was made up to 10 μL with nuclease-free water. Annealing was performed in a thermocycler by running a denaturation cycle at 95°C for 5 min followed by gradual cooling to room temperature at $1^{\circ}\text{C min}^{-1}$. The annealed reaction mixture served as a template for subsequent IVT reactions. The 10 μL annealed reaction was mixed with 10 μL of NTP buffer mix and T7 RNA polymerase mix from the HiScribe T7 Quick High Yield RNA Synthesis Kit (NEB, USA), and the final volume was made up to 40 μL with nuclease-free water. The transcription reaction was incubated at 37°C for 4 h.

The IVT products were purified using RNeasy MinElute Cleanup Kit (QIAGEN, USA) according to the manufacturer's protocol. Purified crRNA was quantified with NanoDrop and the correctness was confirmed by electrophoresis. Aliquots of the crRNA were stored at -20°C to avoid repeated freeze-thawing until further use.

2.5. Pre-amplification and lateral flow assay (LFA)-based detection

Lateral flow detection reactions were set up as described in Gooenberg et al. [32] with some modifications. The detection was carried out as a two-pot SHERLOCK (Specific High Sensitivity Enzymatic Reporter UNLOCKing) reaction, wherein, the basic RPA reaction was first performed following the instructions of the TwistAmp Basic Kit (Twist Dx, United Kingdom). First, each RPA reaction was set up in a reaction volume of 50 μL containing 29.5 μL rehydration buffer, 2.4 μL each of forward and reverse primers (10 μM), and the remaining volume made up with RNase-free water. Then 1–2 μL (50 ng μL^{-1}) input of the

extracted sample was added to each reaction. The reaction mixture was vortexed and spun briefly before adding 2.5 μL of 280 mM magnesium acetate (MgOAc) for the reaction to initiate. The reaction mixture was incubated at 37 °C for 15–20 min in a thermocycler and gently flicked after 5 min since the initiation of the reaction to ensure even substrate distribution. The amplicon generated from the RPA reaction served as the template for *in vitro* transcription using T7 RNA polymerase to generate the *Klebsiella rmpA* gene target.

The SHERLOCK reaction mixture protocol published by Kellner et al. [30] was referred for guidance and then optimized and further modified as described below. As advised, to avoid the possibilities of reagent and work area contamination that may generate false positive signals, separate pre- and post-amplification work areas were used when setting up the RPA and *LwaCas13a* reaction. Before setting up the reaction, the entire surface and the pipettes were wiped down with an RNase-away solution. For the SHERLOCK reaction, CRISPR-Cas reaction mixture was prepared by adding the following components in a microfuge tube in top-down order for a reaction volume of 20 μL : 0.4 μL 1 M HEPES, 0.36 μL 0.5 M MgCl₂, 0.5 μL 1 mg mL⁻¹ purified *LwaCas13a*, 0.5 μL 40U μL^{-1} murine RNase inhibitor, 2 μL 10 mM rNTP solution mix, 2 μL 10X T7 buffer, 0.5 μL 50U mL⁻¹ T7 RNA polymerase, 100 nM *rmpA* crRNA, 1 μL RPA template, 0.2 μL 100 μM LF-RNA reporter and the remaining volume made up with RNase-free water. The reaction was incubated at 37 °C for 50 min.

The end results of the lateral flow reaction were detected on commercially available lateral flow strips (Milenia HybriDetect 1, TwistDx). A custom probe FAM-Biotin polyU RNA reporter (/56-FAM/rUrUrUrUrUrU/3Bio) was synthesized from Integrated DNA Technologies, USA. After the completion of the reaction, Cas13a detection reactions were diluted to 1:5 in Hybridetect 1 Assay Buffer, and the LFA strips were then dipped and incubated at room temperature for 5 min. The strips were then removed from the solution, aired and the results were interpreted.

3. Results

3.1. Cloning and expression of recombinant *LwaCas13a* in *E. coli*

The foremost step was to recombinantly express *LwaCas13a* in *E. coli* followed by purifying the recombinant protein using Ni-NTA affinity chromatography. The clone producing a linearized band of 8.8 kb was taken as the desired clone (SHER10) harbouring *LwaCas13a* gene (Fig. S1). SHER10 was confirmed for correctness through restriction digestion, PCR amplification and DNA sequencing. Following the transformation and expression, chromatography products were analyzed and visualized by denaturing gel electrophoresis, which revealed that induced *E. coli* cells had produced the desired protein with a molecular weight comparable with the predicted *LwaCas13a* weight (~143.7 kDa) (Fig. S2).

3.2. Isothermal pre-amplification of target sequence

A 120-bp fragment of the *rmpA* gene was chosen as the target region specific for *K. pneumoniae* as predicted by the primer-BLAST software. The specificity of RPA primers towards the *rmpA* gene of hypervirulent *K. pneumoniae* (hvKp) was evaluated by setting up RPA reactions under optimized conditions tested across all 18 test strains of *K. pneumoniae*. To assess if the target nucleotide sequence was being amplified specifically through RPA, we first used just one primer pair to confirm amplification. The conditions used at this point for the said amplification were as instructed in the manufacturer's protocol without any further optimization. Prior to performing RPA, the presence of *rmpA* gene across all test strains of *K. pneumoniae* was affirmed through PCR (535 bp) using *rmpA*-PCR/F and *rmpA*-PCR/R primers (Table 1) based on Yeh et al.'s work [33]. Genomic DNA extracted from all 18 *K. pneumoniae* strains served as the template for the PCR amplification. As determined through

PCR, *K. pneumoniae* MTCC KP109 and M59 were found to bear the hypervirulent gene *rmpA* (Fig. S3) and therefore for the subsequent optimization process, strain MTCC KP109 was taken as the positive control and nuclease-free water as the negative control. The appropriateness of RPA was confirmed by running the product on 2 % agarose gel (RPA-AGE), and as it was expected, a band of ~120 bp was observed in the positive control with no significant amplification in the negative control when visualized over a UV-transilluminator.

3.2.1. Primer-set validation and evaluation of optimal conditions

To screen out the most efficient primer set, four different RPA primer pair combinations (*rmpA*-RPA F1R1, F1R2, F2R1 and F2R2) (Table 1) were tested with experimental positive and non-template control (NTC) to determine their aptness in amplifying *rmpA*. All primer combinations were first tested for amplification at 37 °C for 20 min. The products amplified by RPA were electrophoresed on a 2 % agarose gel and observed under a UV lamp. The RPA-AGE results confirmed the amplification of target *rmpA* gene in all possible combinations of primer sets with no non-specific bands in the NTC, however, the optimal amplification was observed in F1R1 combination (Fig. 1a).

The F1R1 primer pair was then optimized in terms of incubation time and temperature and the results were visualized through RPA-AGE. RPA is known to function at the isothermal range of 37–42 °C, and therefore, reactions were carried out at temperatures ranging from 37–43 °C with 1 °C increments. The optimal temperature for this investigation turned out to be 37 °C, as deciphered from the intactness of the band in RPA-AGE, regardless of amplification at all temperatures from 37 to 43 °C (Fig. 1b). Upon exceeding the recommended range of temperature, indeed a decrease in the intensity of the amplified product was observed at 43 °C.

A threshold amplification began to be seen 5 min after the start of the reaction as observed as a faint band which continued till about 30 min (Fig. 1c). Since the intensities of the amplified product at 20 and 30 min were largely the same, amplification at 37 °C for about 20 min was fixed as the optimum duration for RPA reactions of *rmpA*.

In RPA, the amplification was initiated by the addition of MgOAc to the reaction mixture. The suggested MgOAc concentration range for the reaction was 12 mM to 30 mM, the standard concentration being 14 mM. Based on the application notes of the manufacturer, three different concentrations of MgOAc (14 mM, 20 mM and 22.4 mM per pellet) were tested in this study to determine the optimum concentration of MgOAc required to initiate the reaction at the soonest (Fig. 1d). Since, no significant difference in the intensities of the band was observed, the standard concentration of 14 mM MgOAc was accepted for all further RPA reactions.

The F1R1 primer-pair was recognized as the best-suited primer combination and the pair was taken into further consideration in the amplification process. All 18 test strains of *K. pneumoniae* were then amplified through RPA based on these optimised reaction conditions. The specificity of the chosen primer set was also validated by performing an RPA reaction under pre-determined conditions against six other bacteria belonging to different genera, including *E. coli*, *S. aureus*, *P. aeruginosa*, *S. marcescens*, *C. violaceum* and *B. subtilis*. The genomic DNA of these bacteria were used as templates to amplify the *rmpA* gene, however, positive band corresponding to the size of the gene of interest were seen in none signifying that the selected primer set holds distinct specificity for the *rmpA* gene of hvKp and does not cross-react and amplify any other pathogen or the strain of *K. pneumoniae* negative for *rmpA* (Fig. S4).

3.3. Verifying the collateral cleavage activity of *Cas13a* in *K. pneumoniae*

We intended to detect hvKp through means of the CRISPR-Cas13a system. For this assay, the reporter molecules that remained intact, or simply put, those molecules which did not undergo cleavage were captured at the first line of detection, generating a visible band on the

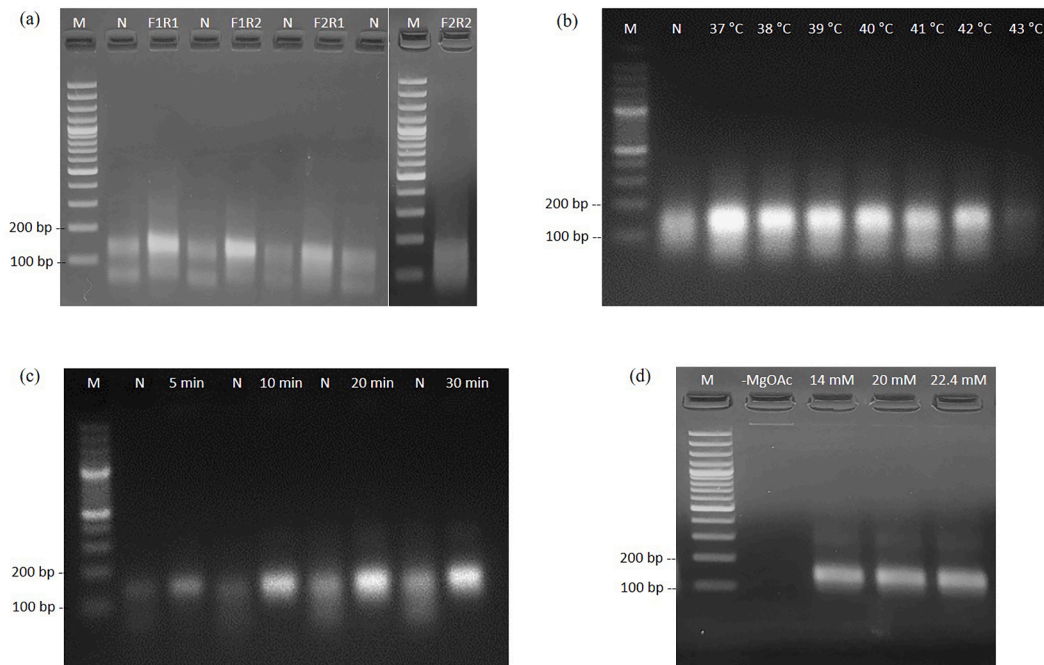


Fig. 1. Primer screening and condition optimization for pre-amplifying *rmpA* using RPA (a) Primer set selection demonstrating each primer set combination (F1R1, F1R2, F2R1, and F2R2) along with its respective NTC as stated above each lane. The band size of the DNA ladder is mentioned on left, (b) The effect of temperature on RPA reaction determined through amplification at varying temperatures ranging from 37–43 °C, (c) Assessing the difference in intensities of the amplified product upon RPA carried over a period of 5–30 min with respect to corresponding NTCs, and lastly (d) Magnesium acetate (MgOAc) concentration optimization through RPA based on F1R1 primer pair; the first lane represents an RPA reaction without the addition of MgOAc and the subsequent lanes demonstrates the effect on RPA following the addition of 2.5, 3.6 and 4.0 mM MgOAc. *M* molecular marker, *N* non-template control.

control line, and therefore were considered negative. Only those samples that generated a signal at the second line of detection (test line) were considered positive for this test.

3.3.1. Species-specific detection of *K. pneumoniae* test strains

In order to verify the feasibility and specificity of the collateral cleavage functionality of recombinant *LwaCas13a* in detecting

K. pneumoniae in general, the assay was first tested upon the species-specific *K. pneumoniae rpoB* gene which was initially chosen as the target sequence. The *rpoB* actually encodes the β -subunit of bacterial RNA polymerase and every bacterial species possesses this gene, but the length and nucleotide sequence of this gene in different bacteria is somewhat different [34]. The *rpoB* is therefore considered a crucial determinant for the identification of different bacterial species and

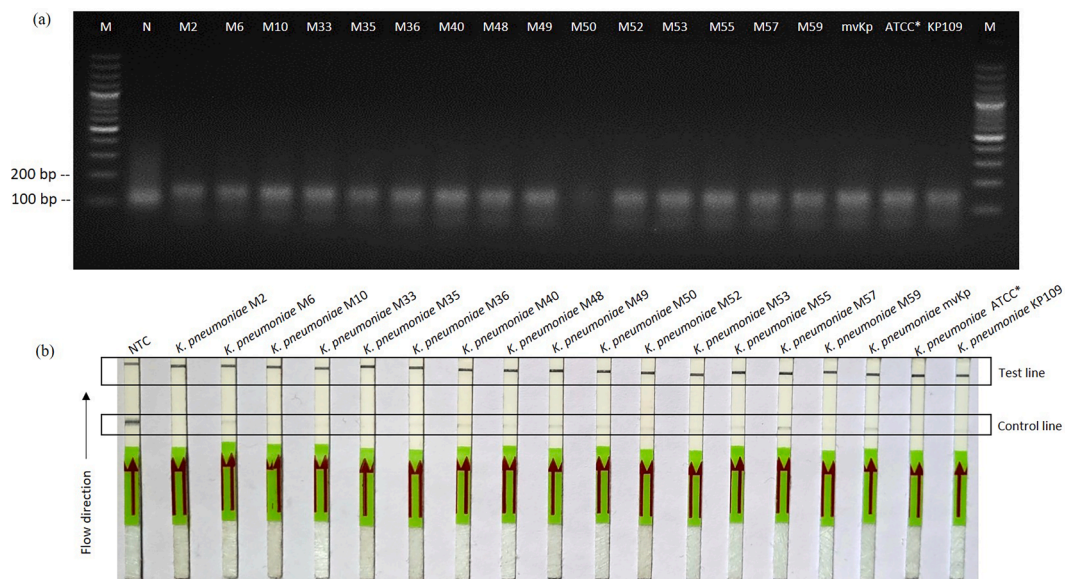


Fig. 2. (a) Amplification of *rpoB* performed on all 18 test strains of *K. pneumoniae*. It demonstrates the RPA-AGE image of the amplified products of the *rpoB* gene, (b) Lateral flow assay for species-specific detection of *K. pneumoniae*. LFA was performed on 18 clinical test strains of *K. pneumoniae* flow assay for determining the species-specific presence of *rpoB*. When visualized in the direction of flow, appearance of the first band (control line) denotes non-cleavage of reporter, while development of the second band (test line) signifies reporter cleavage and therefore target detection. All the test strains of *K. pneumoniae* tested positive for the presence of *rpoB*. *ATCC**, *K. pneumoniae* ATCC1705.

analyzing phylogeny, especially when studying closely related isolates [35]. For this, a two-pot SHERLOCK detection approach was opted. The target DNA sequence for the *rpoB* gene from all 18 *K. pneumoniae* test strains were amplified in advance through RPA (191 bp) (*rpoB*-RPA/F and *rpoB*-RPA/R primers (Table 1)) and used as the template for the *LwaCas13a* detection assay (Fig. 2a). Following an hour of incubation of the reaction at 37 °C, the reaction was diluted with 80 μ L hybridetect assay buffer supplied with the LFA kit. In the case of *rpoB*, a distinctly visible red-coloured band was observed in all of the test isolates of *K. pneumoniae* ensuring genuine and accurate detection of *K. pneumoniae* (Fig. 2b). No such band was observed on the control line, suggesting no capturing of intact reporter molecules because of their collateral cleavage as a function of *LwaCas13a*. A control band was observed in the NTC without a distinctly perceivable test band indicating the absence of *K. pneumoniae*-specific *rpoB* gene in the sample.

3.3.2. Hypervirulence detection of *K. pneumoniae* test strains

Once the feasibility of the detection system was ensured, the confirmed strains of *K. pneumoniae* were examined for the presence of *K. pneumoniae*-specific *rmpA* gene. The RPA-based amplification of all 18 test strains of *K. pneumoniae* based on the optimized reaction conditions were visualized on RPA-AGE as shown in Fig. 3a. For LFA-based detection, a band at the first line of detection was taken as negative for *rmpA* and the appearance of a band at the second line of detection was considered positive for *rmpA*. Red bands were observed on the test line of isolates M59 and KP109 indicating the presence of *rmpA* gene (Fig. 3b). This asserts the specific detection of *rmpA* which encodes a unique peptide of 25 kDa and is strongly associated with *K. pneumoniae*'s hypermucoviscosity phenotype in human isolates [36]. This result was in agreement with the RPA-AGE image (Fig. 3a) wherein amplification of the *rmpA* fragment was observed in only the said two strains.

3.4. Cross-reactivity validation across different genera

To validate the selectivity of the CRISPR detection assay towards *K. pneumoniae*-specific genes, the assay was performed on six different genera of bacteria including *E. coli*, *S. aureus*, *P. aeruginosa*, *S. marcescens*, *C. violaceum* and *B. subtilis*, and test the cross-reactivity of the CRISPR detection tool. In this test, *K. pneumoniae* ATCC1705 was

used as the positive control and for the NTC, nuclease-free water was used as the template. Three other already screened strains of *K. pneumoniae* reported in this study, namely strains M2, M59 and KP109 were randomly picked to test and compare the results across different genera. As mentioned in previous sections, pre-amplified RPA products of the listed organisms were used as templates for detection. The CRISPR-based *rpoB* detection assay showed, no cross-reactivity towards the DNA of any of the alternate pathogens in the study except for *K. pneumoniae* strains, i.e. ATCC KP1705, M2, M59 and KP109, leading to clear identification of *K. pneumoniae* strains, and therefore was assured to be specific for the target (Fig. 4a). The same strains were then tested for the presence of *rmpA* across different genera. In the cross-reactivity testing for the detection of *rmpA*, positive results were only observed in strains KP109 and M59 (Fig. 4b). Appearance of just the test band was observed in none of the non-specific target bacteria, indicating that the assay was negative for those and selective for *rmpA*-specific strains only.

3.5. Sensitivity assay of the RPA-LFA

To determine the sensitivity or the minimum detection limit of the CRISPR-assisted detection assay for detecting *rmpA*, serial dilutions of nucleic acid of *K. pneumoniae* strains were used. We started with an initial concentration of 1025 ng μ L⁻¹ of genomic DNA of *K. pneumoniae* KP109 as read on UV spectrophotometer, and then serially diluted the genomic DNA at the gradient of 10⁻¹, 10⁻², 10⁻³, 10⁻⁴, 10⁻⁵, 10⁻⁶, 10⁻⁷, and 10⁻⁸ dilutions, which were used as templates for subsequent reactions. The diluted DNA was amplified using RPA, followed by the Cas13a-LFA detection. The minimum limit of detection (LOD) was realised to be at the dilution of 10⁻⁵ which concentration-wise corresponded to 10.25 pg μ L⁻¹ of genomic DNA. The band on the control line appears to fade gradually with an increase in the concentration of the template (Fig. 5).

4. Discussion

K. pneumoniae is a major causative pathogen of opportunistic healthcare-associated infections globally, poses a great threat to the community which in turn is increasingly aggravated by the prevalence

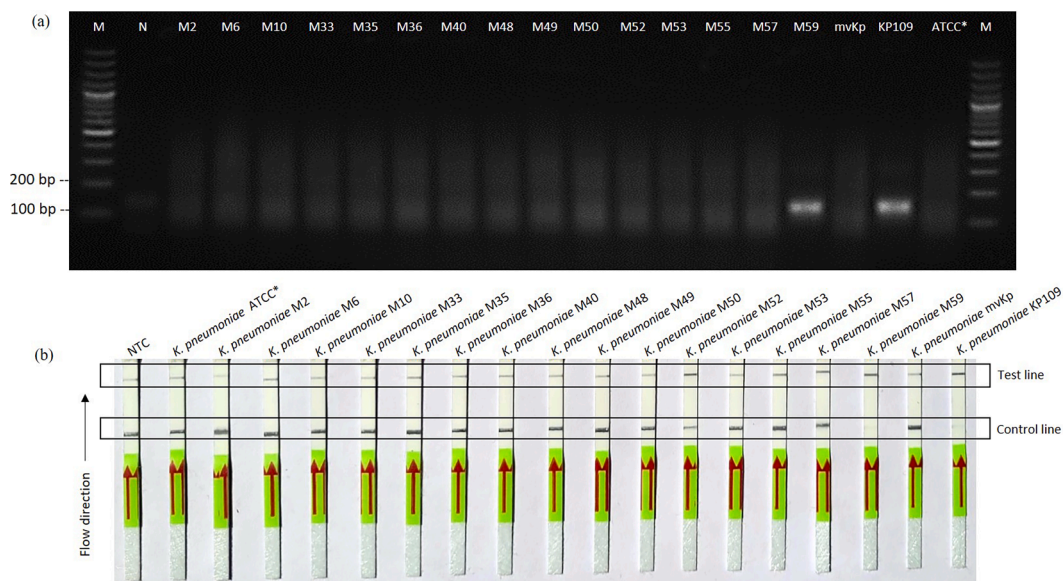


Fig. 3. (a) Amplification of *rmpA* under pre-optimized conditions performed on all 18 test strains of *K. pneumoniae*. Figure demonstrates the RPA-AGE image of the amplified products of the *rmpA* gene, (b) LFA for determining the hypervirulent form of *K. pneumoniae*. LFA for determining the hypervirulent form of *K. pneumoniae* for detecting the presence of *rmpA*. In line with the data of RPA image of *rmpA* amplification, two of the test strains, namely *K. pneumoniae* M59 and KP109 were tested positive for the presence of *rmpA*.

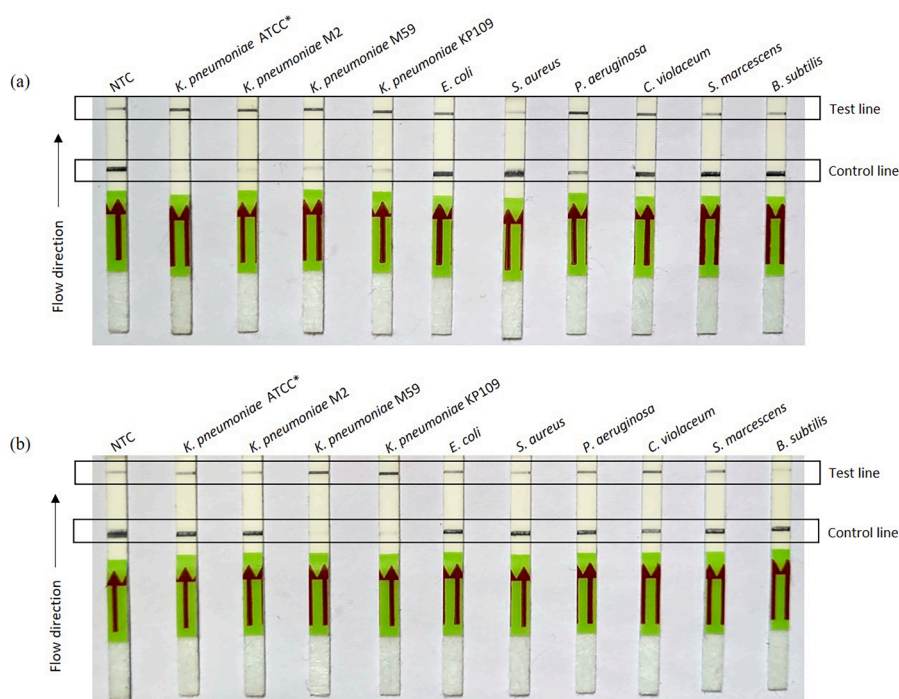


Fig. 4. Validation of CRISPR-assisted diagnostic tool for specificity and cross-reactivity across genera. (a) *rpoB* detection based on CRISPR-assisted LFA, (b) *rmpA* detection based on CRISPR-assisted LFA.

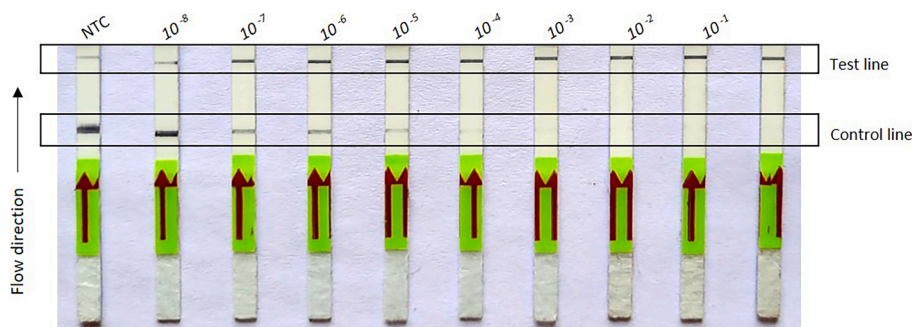


Fig. 5. LFA results demonstrating the testing of minimum limit of detection for *Klebsiella*-specific *rmpA*. The amount added to the RPA reaction (ng/mL) is shown at the top of each lane. Lanes with a distinctly brighter test band against the control band were considered to be favouring the test (concentration $1-10^{-5}$).

of extended-spectrum beta-lactamases (ESBLs) and carbapenem resistance. The organism is capable of acquisition of numerous virulence factors by the exchange of foreign mobile genetic elements further adding up to its noxious characteristics and evading host-immune response. The bacteria can thrive in a variety of environmental niches due to metabolic versatility and so are frequent colonisers of mucosal surfaces (i.e. intestine, upper respiratory tract and urinary tract). The pathogen is known for its high degree of plasticity and as a virtue of that possesses the ability to acquire virulent and resistance-conferring plasmids [37]. The predominant modes of virulence in *K. pneumoniae* are attributed to the factors of enhanced lipopolysaccharide synthesis and polysaccharide capsules formation, along with fimbrial adhesion and siderophore production [37,38]. The thick capsule and biofilm endow the bacteria with high-level resistance to escape the host immune surveillance by obstructing the access of antibodies and antibacterial peptides to the inside of the cell [39]. In the interior core of the biofilm-protected cells, the bacteria adapt to starvation and that along with low oxygen availability arrests the growth, thereby diminishing the efficacy of antibiotics to act on metabolically active and dividing cells [40,41]. *K. pneumoniae* biofilms that develop on the inner surfaces of catheters and other indwelling devices are the most clinically significant

[42]. Patients with impaired immune systems are more susceptible to the prevalence of *K. pneumoniae* biofilms which may very likely aid in the colonisation of the gastrointestinal, respiratory and urinary tracts and eventually lead to the emergence of invasive infections. *K. pneumoniae*'s involvement in causing meningitis, pulmonary pneumonia, UTIs, abdominal infections, bacteremia, septicemia and pyogenic liver abscess in immunocompromised as well as healthy individuals have been reported [43–46].

The global market for infectious disease diagnostics rallied at USD 35.5 billion in 2022, and is projected to witness a slight decrease of -1.4 % CAGR hitting 33.1 billion USD by 2027, considering a decline in the number of reported cases of COVID-19 [47]. Nevertheless, increased awareness for early disease detection, a shift in prioritising the need to move centralised laboratories to decentralise POC testing, and technical advancements are all proving to be driving factors for the market's consistency. In a recent article published in Nature, it was reckoned that CRISPR-based diagnostics rank among seven promising technologies to stand out in 2022 [48]. CRISPR-based diagnostics work much faster than culture-based identification methods, as compared to PCR-based testing, it allows amplification to happen isothermally, thereby minimizing or nearly abandoning the dependency on specialized instruments. In

K. pneumoniae, enhanced *rmpA* production leads to the emergence of hypermucoviscous phenotype and transcriptional fusions of csp-promoter regions tend to increase in expression in the presence of excess *rmpA* [49]. The presence of virulence-causing *rmpA* gene is mainly determined through the PCR [50] and/or MALDI-TOF MS [51] methods which are instrument-dependent and are not suitable for rapid diagnosis. These processes are also labour-intensive, lengthy and rely heavily on sophisticated instruments. Isothermal amplification processes, particularly RPA, can steer clear of the usage of any complex machinery and also carry out amplification in a temperature range of 37–42 °C, thereby defining its suitability for rapid on-site applications.

The two-pot CRISPR-based nucleic acid detection platform contrived in this study aimed for the rapid and accurate recognition of *K. pneumoniae* species and distinguish the hypervirulent *K. pneumoniae* out of the pool of already detected *K. pneumoniae*. A number of studies have used *rpoB* for the identification of *K. pneumoniae* [52–54]. It is said that the hypervariable region of this gene, which is located between positions 2300 and 3300, is the most suited for identification and phylogenetic discrimination at the species and subspecies level [35]. The CRISPR-assisted *K. pneumoniae* detection assay was extremely specific for *K. pneumoniae* and efficiently identified all of the 18 strains of *K. pneumoniae* and achieved 100 % inclusivity and exclusivity applied to various pathogens (Table 2). Amplification of the target sequence was first visualized and ensured for correctness by running the resultant amplicon on AGE. We did not observe any sort of false-positive detection in this assay. From the diagnostics perspective, this assay gives instrument-free read-outs, performs at 37 °C and gets done in just two fluid-handling steps. The target-dependent crRNA designed for the genes *rpoB* and *rmpA* are to be credited for the dependability and accuracy of this CRISPR-based detection platform. An upper hand of using LFA-based detection is that the users can visualize the development of bands on their own with naked eyes and interpret accordingly based on instructions guided regarding the development of subsequent bands. Due to its reduced cost and user-friendly nature, LFA for nucleic acid detection has drawn more interest as the need for diagnosis in environments with limited resources. However, no technology is perfect and therefore with CRISPR-based LFA-based detection too, there exists a constraint. Despite the quickness, simplicity, stability, and visual qualities of LFA, it lacks the sensitivity necessary to detect important markers that are present in incredibly small concentrations in a sample, which limits the applications that can be made of them. A bottleneck of LFA-based fluorescence detection is the LOD. With increase in dilution, the LOD tends to diminish, which in our case implies that the collateral cleavage function of the Cas13a remained dormant since the crRNA for *rmpA* did not find the target nucleotide sequence (because of sparsely available targets) and therefore could not bind to the target strand. Also, to be recognized as a useful POC diagnostic, a diagnostic tool under development needs to be thoroughly tested on a variety of clinical samples and situations. This is especially important for treating acute infections. Although most of the *Klebsiella* strains examined in this investigation were obtained as isolates from blood and urine specimens, we did not really test the developed diagnostic tool directly on biological fluids that were potentially contaminated. An inclusive study of this sort might have offered greater clarity of the tool's overall effectiveness in its current version.

Cutting down multiple liquid handling steps and manual operations readily simplifies the process of detection, minimizes the chances of cross-contamination and streamlines the detection process for early detection and timely therapeutic intervention concerned with *K. pneumoniae* infections. Also, simplifying diagnostic procedures will make it much easier to bring analyses near bedside to be handled by less-trained personnel by following straightforward instructions. This will not only democratize access to healthcare but also lessen the burden on healthcare centres and overworked medical personnel. Unfortunately, despite the knowledge of the fact that consequences from infectious illness are directly correlated with a prolonged pathogen identification

Table 2
A symbolic summary of the detection results obtained in this study.

LFA results		Species-specific diagnostics																		Cross-reactivity testing						
Target	NTC	M2	M6	M10	M33	M35	M36	M40	M48	M49	M50	M52	M53	M55	M57	M59	KPMV 36808	ATCC 1705	MTCC KP109	EC	SA	PA	CV	SM	BS	
<i>rpoB</i>	×	✓	✓	✓	✓	✓	✓	✓	✓	✓	✓	✓	✓	✓	✓	✓	✓	✓	✓	×	×	×	×	×	×	×
<i>rmpA</i>	×	×	×	×	×	×	×	×	×	×	×	×	×	×	×	×	×	×	×	×	×	×	×	×	×	×

NTC non-template control, KP *Klebsiella pneumoniae*, EC *Escherichia coli*, SA *Staphylococcus aureus*, PA *Pseudomonas aeruginosa*, CV *Chromobacterium violaceum*, SM *Serratia marcescens*, BS *Bacillus subtilis*.

process which only adds to aggravation of the infectious state, conventional hospital laboratories are still constrained by slow, multistep culture-based assays, which delays therapeutic care in acute and critical-care settings. This only aids the bacteria to establish a full-fledged infection. It is envisaged that this technology may take the shape of a futuristic diagnostic tool wherein individuals may test any of their biological secretions swabbed from urine, saliva, or nasal lining, in the comfort of home. An instrument-free mode of result readout would allow them to observe and interpret outcomes by following a simple instruction booklet [55].

Piepenburg et al. [56] published their initial findings of the RPA in a paper entitled "DNA Detection Using Recombination Proteins" and they were already cognizant of the value of their revolutionary DNA amplification technique for POC applications. After 17 years the publication of this seminal study, RPA still is amongst the most widely utilized isothermal DNA-amplification techniques. But just as no technology in this world is flawless, RPA is not either. A significant shortcoming of RPA, in addition to the issue of potential carryover contaminations, is the non-specific amplification of undesirable products. RPA reactions do generate some amount of background noise, wherein the resultant products rarely get sequenced. These artefacts may possibly arise as a result of undesired interaction of the primers and may sequentially cumber the desired amplification by unnecessarily consuming primers and crowding around the assay's resources [57]. Usually, RPA primers are quite lengthy (28–35 nt), and with no steps involving temperature denaturation of DNA, the likelihood of the labelled RPA primers cross-dimerizing is high, which could be a reason why cross-dimers can provide misleading positive signals [58]. Such artefacts may themselves serve as templates for subsequent amplification cycles and thus enter into an unavoidable phase of exponential amplification. During the initial course of this study, we were skeptical of RPA results, but fortunately, we stumbled upon Rani et al.'s [59] work on RPA-based LFA bioassay designed for *E. coli* and realized that our results were not actually erroneous. The non-specific products take up the stains of the DNA dyes which could be a reason for the sheared effect observed in the non-target strains. Piepenburg et al. [56] had anticipated this flaw of the RPA method and suggested incorporating an additional enzyme endonuclease IV (nfo) into the RPA reaction to overcome the issue of non-specific amplification. TwistDx, the company that primarily supplies RPA reagents used to supply a kit by the name of TwistAmp® nfo kit for this purpose. However, since 2022, this kit has been discontinued, and thus if needed, one has to make their own version by simply mixing endonuclease IV with the TwistAmp® Basic Kit. Since the RPA kit that we used in our study was just the TwistAmp® Basic Kit, the background noise may have arrived for that particular reason. A thorough investigation of the same could be found in Tan et al.'s [16] work wherein the authors have beautifully compiled the pros and cons of RPA. We must acknowledge the fact that RPA does give some amount of background amplifications and it may give false-positive results. Amalgamating technologies or approaches, for instance CRISPR that bring in specificity to this isothermal amplification technique is sure to take the success of this tool a notch further.

Similar to this study, Li et al. [60] demonstrated the detection of *rmpA2* gene through an RPA-LFA-based detection protocol without involving CRISPR-Cas systems. Interestingly, in a quest to find out what beneficial effect CRISPR may offer to this detection process, especially when detection is also possible through RPA-LFA method, we came across work by Zhou et al. [61]. The study was based upon the detection of *S. aureus* from food samples and the authors discussed why Cas13a is a better choice of nuclease than its coequal counterpart Cas12. The reasons were as follows: 1) Cas13a was found to be more active in delineating collateral cleavage activity as compared to Cas12, thus resulting in enhanced fluorescence. 2) Cas12 requires dsDNA or ssDNA as the substrate which technically means that a target DNA molecule does not need to be transcribed into an RNA strand for detection, as in the case of Cas13 [62]. Zhou et al. [61] found that inclusion of the transcription

step generates a lot more number of target sequences, resulting in better sensitivity and considerably lower LOD (1 CFU mL⁻¹ of *S. aureus* for Cas13a as against 10³ CFU mL⁻¹ in the case of Cas12a). 3) Most importantly, this detection platform can leverage the potential of CRISPR type III effector nuclease Csm6, which is a single strand-specific endoribonuclease that can work in tandem with Cas13a to accelerate the collateral cleavage activity and intensify trans-cleavage signal sensitivity [63]. This is not possible with Cas12a. RPA alone can produce background signals which may lead to false-positive detection. However, by bringing CRISPR to this scenario, one can harness the specificity of the crRNA which is the crux of this technology.

Given how quickly *K. pneumoniae* may transform from a typical gut commensal to a hypervirulent bug, early detection of biothreat agents, for instance, hvKp in this case, using highly proficient and ultra-specific diagnostic tools could evade possibilities of an outbreak of epidemic in the community. However, it is easier said than done when it comes to conceiving POC tools since the practical and regulatory sanctions decelerate or sometimes even impede the transition of laboratory tests for on-site applications. It goes without saying that when using POC devices compliance with federal, state and local regulations must be met. Operational turn-around time is a critical aspect of consideration for any novel POC to prove its applicability and therefore it is important that the assay must hold relevance to the current gold standards of testing. Stability of the crRNA is yet another key element of efficient CRISPR-assisted diagnostics. Extrinsic influences such as nucleases could be causing crRNA degradation by affecting its stability and integrity, thereby impeding pathogen detection. Besides, it is also important to ensure that the Cas13 nuclease doesn't lose its effectiveness due to factors such as storage conditions, incorporation of cryoprotectants, concentration of buffers and salts, pH, lyophilization and several other factors that could leave significant effects on biomolecule stability and activity. With time, as the CRISPR-assisted POC technologies continue to mature, such issues could be systematically addressed and resolved in order to realize their benefits for the routine care of patients.

5. Conclusion

The CRISPR-based diagnostic approach demonstrated in this study presents a promising solution for rapid and accurate species-specific detection of *K. pneumoniae*. The assay was completed in a span of 1 h and 10 min (50 min of CRISPR reaction, 15 min of RPA and 5 min of LFA) at a constant temperature of 37 °C without the need for any specific instrumentation. The compatibility of this diagnostic tool with paper-based LFA formats enhances its accessibility, making it easily interpretable even by individuals without specialized training. This CRISPR-based diagnostic tool could be very useful for rapid and accurate diagnosis of *K. pneumoniae* infection, especially in resource-limited settings. Persistent efforts invested in this area could facilitate outstretching the tool to field-level for on-the-spot applications where costly instrumentation is inaccessible or in compromised-resources settings, which will lessen the dependence on sample collection, transportation and testing in laboratories.

CRedit authorship contribution statement

Gargi Bhattacharjee: Writing – review & editing, Writing – original draft, Software, Methodology, Investigation, Formal analysis, Data curation. **Nisarg Gohil:** Writing – review & editing, Formal analysis. **Khushal Khambhati:** Writing – review & editing, Formal analysis. **Devarshi Gajjar:** Writing – review & editing, Resources. **Ali Abusharha:** Writing – review & editing. **Vijai Singh:** Writing – review & editing, Supervision, Funding acquisition, Conceptualization.

Declaration of competing interest

The authors declare that they have no known competing financial

interests or personal relationships that could have appeared to influence the work reported in this paper.

Data availability

No data was used for the research described in the article.

Acknowledgements

G.B. and K.K. acknowledge the Indian Council of Medical Research of the Government of India for financial assistance in the form of a Senior Research Fellowship (File No. 5/3/8/41/ITR-F/2022-ITR and AMR/Fellowship/36/2022-ECD-II, respectively). Financial assistance from Gujarat State Biotechnology Mission (GSBTM Project ID - 5LY45F), Government of Gujarat, India to V.S. is acknowledged. A.A. extends his appreciation to the Researchers Supporting Project number (RSPD2024R653), King Saud University, Riyadh, Saudi Arabia.

Appendix A. Supplementary data

Supplementary data to this article can be found online at <https://doi.org/10.1016/j.microc.2024.110931>.

References

- [1] D.S. Chertow, Next-generation diagnostics with CRISPR, *Science* 360 (2018) 381–382, <https://doi.org/10.1126/science.aat4982>.
- [2] C.J. Murray, K.S. Ikuta, F. Sharara, L. Swetschinski, G.R. Aguilar, A. Gray, C. Han, C. Bisignano, P. Rao, E. Wool, Global burden of bacterial antimicrobial resistance in 2019: a systematic analysis, *The Lancet* 399 (2022) 629–655, [https://doi.org/10.1016/S0140-6736\(21\)02724-0](https://doi.org/10.1016/S0140-6736(21)02724-0).
- [3] CDC, AR Threats Report, 2021. <https://www.cdc.gov/drugresistance/biggest-threats.html>. (Accessed 27.10.2023).
- [4] CDC, COVID-19 & Antimicrobial Resistance, 2022. <https://www.cdc.gov/drugresistance/covid19.html>. (Accessed 27.10.2023).
- [5] H.W. Boucher, G.H. Talbot, J.S. Bradley, J.E. Edwards, D. Gilbert, L.B. Rice, M. Scheld, B. Spellberg, J. Bartlett, Bad bugs, no drugs: no ESKAPE!, *An Update from the Infectious Diseases Society of America*, *Clin Infect Dis* 48 (2009) 1–12, <https://doi.org/10.1086/595011>.
- [6] S.S. Magill, J.R. Edwards, W. Bamberg, Z.G. Beldavs, G. Dumyati, M.A. Kainer, R. Lynfield, M. Maloney, L. McAllister-Hollod, J. Nadle, S.M. Ray, D.L. Thompson, L. E. Wilson, S.K. Fridkin, I. Emerging Infections Program Healthcare-Associated, T. Antimicrobial Use Prevalence Survey, Multistate point-prevalence survey of health care-associated infections, *N Engl J Med* 370 (2014) 1198–208.
- [7] R. Selden, S. Lee, W.L. Wang, J.V. Bennett, T.C. Eickhoff, Nosocomial klebsiella infections: intestinal colonization as a reservoir, *Ann Intern Med* 74 (1971) 657–664, <https://doi.org/10.7326/0003-4819-74-5-657>.
- [8] C.L. Gorrie, M. Mirceta, R.R. Wick, L.M. Judd, M.M.C. Lam, R. Gomi, I.J. Abbott, N. R. Thomson, R.A. Strugnell, N.F. Pratt, J.S. Garlick, K.M. Watson, P.C. Hunter, D. V. Pilcher, S.A. McGloughlin, D.W. Spelman, K.L. Wyres, A.W.J. Jenney, K.E. Holt, Genomic dissection of Klebsiella pneumoniae infections in hospital patients reveals insights into an opportunistic pathogen, *Nat Commun* 13 (2022) 3017, <https://doi.org/10.1038/s41467-022-30717-6>.
- [9] N. Petrosillo, M. Giannella, R. Lewis, P. Viale, Treatment of carbapenem-resistant Klebsiella pneumoniae: the state of the art, *Expert Rev Anti Infect Ther* 11 (2013) 159–177, <https://doi.org/10.1586/eri.12.162>.
- [10] R. Podschun, U. Ullmann, Klebsiella spp. as nosocomial pathogens: epidemiology, taxonomy, typing methods, and pathogenicity factors, *Clin Microbiol Rev* 11 (1998) 589–603, <https://doi.org/10.1128/CMR.11.4.589>.
- [11] U. Okomo, E.N.K. Akpalu, K. Le Doare, A. Roca, S. Cousens, A. Jarde, M. Sharland, B. Kampmann, J.E. Lawn, Aetiology of invasive bacterial infection and antimicrobial resistance in neonates in sub-Saharan Africa: a systematic review and meta-analysis in line with the STROBE-NI reporting guidelines, *Lancet Infect Dis* 19 (2019) 1219–1234, [https://doi.org/10.1016/S1473-3099\(19\)30414-1](https://doi.org/10.1016/S1473-3099(19)30414-1).
- [12] K. Sands, M.J. Carvalho, E. Portal, K. Thomson, C. Dyer, C. Akpulu, R. Andrews, A. Ferreira, D. Gillespie, T. Hender, K. Hood, J. Mathias, R. Milton, M. Nieto, K. Taiyari, G.J. Chan, D. Bekele, S. Solomon, S. Basu, P. Chattopadhyay, S. Mukherjee, K. Irengu, F. Modibbo, S. Uwaezuoke, R. Zahra, H. Shirazi, A. Muhammad, J.B. Mazarati, A. Rucogozza, L. Gaju, S. Mehtar, A.N.H. Bulabula, A. Whitelaw, B. Group, T.R. Walsh, Characterization of antimicrobial-resistant Gram-negative bacteria that cause neonatal sepsis in seven low- and middle-income countries, *Nat Microbiol* 6 (2021) 512–523, <https://doi.org/10.1038/s41564-021-00870-7>.
- [13] A. Abdeta, A. Bitew, S. Fentaw, E. Tsige, D. Assefa, T. Lejisa, Y. Kefyalew, E. Tigabu, M. Evans, Phenotypic characterization of carbapenem non-susceptible gram-negative bacilli isolated from clinical specimens, *PLoS One* 16 (2021) e0256556.
- [14] A.S. Keshta, N. Elamin, M.R. Hasan, A. Perez-Lopez, D. Roscoe, P. Tang, M. Suleiman, Evaluation of rapid immunochromatographic tests for the direct detection of extended spectrum beta-lactamases and carbapenemases in enterobacteriales isolated from positive blood cultures, *Microbiol Spectr* 9 (2021) e0078521.
- [15] Y. Huang, J. Li, Q. Wang, K. Tang, C. Li, Rapid detection of KPC-producing Klebsiella pneumoniae in China based on MALDI-TOF MS, *J Microbiol Methods* 192 (2022) 106385, <https://doi.org/10.1016/j.mimet.2021.106385>.
- [16] M. Tan, C. Liao, L. Liang, X. Yi, Z. Zhou, G. Wei, Recent advances in recombinase polymerase amplification: Principle, advantages, disadvantages and applications, *Front Cell Infect Microbiol* 12 (2022) 1019071, <https://doi.org/10.3389/fcimb.2022.1019071>.
- [17] R. Kundar, K. Gokarn, CRISPR-Cas System: A Tool to Eliminate Drug-Resistant Gram-Negative Bacteria, *Pharmaceuticals (basel)* 15 (2022), <https://doi.org/10.3390/ph15121498>.
- [18] N. Gohil, G. Bhattacharjee, N.L. Lam, S.D. Perli, V. Singh, CRISPR-Cas systems: Challenges and future prospects, *Prog Mol Biol Transl Sci* 180 (2021) 141–151, <https://doi.org/10.1016/bs.pmbts.2021.01.008>.
- [19] K. Khambhati, G. Bhattacharjee, N. Gohil, G.K. Dhanoa, A.P. Sagona, I. Mani, N. L. Bui, D.T. Chu, J.K. Karapurkar, S.H. Jang, H.Y. Chung, R. Maurya, K. J. Alzahrani, S. Ramakrishna, V. Singh, Phage engineering and phage-assisted CRISPR-Cas delivery to combat multidrug-resistant pathogens, *Bioeng Transl Med* 8 (2023) e10381.
- [20] K. Khambhati, N. Gohil, G. Bhattacharjee, V. Singh, Development and challenges of using CRISPR-Cas9 system in mammals, in: V. Singh, P.K. Dhar (Eds.), *Genome Engineering via CRISPR-Cas9 System*, Elsevier, 2020, pp. 83–93.
- [21] G. Bhattacharjee, N. Gohil, K. Khambhati, I. Mani, R. Maurya, J.K. Karapurkar, J. Gohil, D.T. Chu, H. Vu-Thi, K.J. Alzahrani, P.L. Show, R.M. Rawal, S. Ramakrishna, V. Singh, Current approaches in CRISPR-Cas9 mediated gene editing for biomedical and therapeutic applications, *J Control Release* 343 (2022) 703–723, <https://doi.org/10.1016/j.jconrel.2022.02.005>.
- [22] G. Bhattacharjee, K. Khambhati, N. Gohil, V. Singh, Programmable removal of bacterial pathogens using CRISPR-Cas9 system, in: V. Singh, P.K. Dhar (Eds.), *Genome Engineering via CRISPR-Cas9 System*, Elsevier, 2020, pp. 39–44.
- [23] G. Bhattacharjee, I. Mani, N. Gohil, K. Khambhati, D. Braddick, H. Pancharasa, V. Singh, CRISPR technology for genome editing, in: J. Faintuch, S. Faintuch (Eds.), *Precision medicine for investigators, practitioners and providers*, Elsevier2020, pp. 59–69.
- [24] V. Singh, N. Gohil, R. Ramirez Garcia, D. Braddick, C.K. Fofie, Recent Advances in CRISPR-Cas9 Genome Editing Technology for Biological and Biomedical Investigations, *J Cell Biochem* 119 (2018) 81–94, <https://doi.org/10.1002/jcb.26165>.
- [25] X. Sun, Y. Wang, L. Zhang, S. Liu, M. Zhang, J. Wang, B. Ning, Y. Peng, J. He, Y. Hu, Z. Gao, CRISPR-Cas9 Triggered Two-Step Isothermal Amplification Method for E. coli O157:H7 Detection Based on a Metal-Organic Framework Platform, *Anal Chem* 92 (2020) 3032–3041, <https://doi.org/10.1021/acs.analchem.9b04162>.
- [26] G. Bhattacharjee, N. Gohil, N.L. Lam, V. Singh, CRISPR-based diagnostics for detection of pathogens, *Prog Mol Biol Transl Sci* 181 (2021) 45–57, <https://doi.org/10.1016/bs.pmbts.2021.01.013>.
- [27] Y. Liu, H. Liu, G. Yu, W. Sun, M. Aizaz, G. Yang, L. Chen, One-tube RPA-CRISPR Cas12a/Cas13a rapid detection of methicillin-resistant *Staphylococcus aureus*, *Anal Chim Acta* 1278 (2023) 341757, <https://doi.org/10.1016/j.aca.2023.341757>.
- [28] R. Lei, L. Li, P. Wu, X. Fei, Y. Zhang, J. Wang, D. Zhang, Q. Zhang, N. Yang, X. Wang, RPA/CRISPR/Cas12a-based on-site and rapid nucleic acid detection of *Toxoplasma gondii* in the environment, *ACS Synth Biol* 11 (2022) 1772–1781, <https://doi.org/10.1021/acssynbio.1c00620>.
- [29] H.R. Cheng, N. Jiang, Extremely rapid extraction of DNA from bacteria and yeasts, *Biotechnol Lett* 28 (2006) 55–59, <https://doi.org/10.1007/s10529-005-4688-z>.
- [30] M.J. Kellner, J.G. Koob, J.S. Gootenberg, O.O. Abudayyeh, F. Zhang, SHERLOCK: nucleic acid detection with CRISPR nucleases, *Nat Protoc* 14 (2019) 2986–3012, <https://doi.org/10.1038/s41596-019-0210-2>.
- [31] S.H. Sternberg, R.E. Haurwitz, J.A. Doudna, Mechanism of substrate selection by a highly specific CRISPR endoribonuclease, *RNA* 18 (2012) 661–672, <https://doi.org/10.1261/rna.030882.111>.
- [32] J.S. Gootenberg, O.O. Abudayyeh, J.W. Lee, P. Essletzbichler, A.J. Dy, J. Joung, V. Verdine, N. Donghia, N.M. Daringer, C.A. Freije, C. Myhrvold, R. P. Bhattacharyya, J. Livny, A. Regev, E.V. Koonin, D.T. Hung, P.C. Sabeti, J. J. Collins, F. Zhang, Nucleic acid detection with CRISPR-Cas13a/C2c2, *Science* 356 (2017) 438–442, <https://doi.org/10.1126/science.aam9321>.
- [33] K.M. Yeh, A. Kurup, L.K. Sit, Y.L. Koh, C.P. Fung, J.C. Lin, T.L. Chen, F.Y. Chang, T. H. Koh, Capsular serotype K1 or K2, rather than magA and rmpA, is a major virulence determinant for *Klebsiella pneumoniae* liver abscess in Singapore and Taiwan, *J Clin Microbiol* 45 (2007) 466–471, <https://doi.org/10.1128/JCM.01150-06>.
- [34] E. Andre, L. Goeminne, A. Cabibbe, P. Beckert, B. Kabamba Mukadi, V. Mathys, S. Gagneux, S. Niemann, J. Van Ingen, E. Cambau, Consensus numbering system for the rifampicin resistance-associated rpoB gene mutations in pathogenic mycobacteria, *Clin Microbiol Infect* 23 (2017) 167–172, <https://doi.org/10.1016/j.cmi.2016.09.006>.
- [35] T. Adekambi, M. Drancourt, D. Raoult, The rpoB gene as a tool for clinical microbiologists, *Trends Microbiol* 17 (2009) 37–45, <https://doi.org/10.1016/j.tim.2008.09.008>.
- [36] C.T. Fang, S.Y. Lai, W.C. Yi, P.R. Hsueh, K.L. Liu, S.C. Chang, *Klebsiella pneumoniae* genotype K1: an emerging pathogen that causes septic ocular or

- central nervous system complications from pyogenic liver abscess, *Clin Infect Dis* 45 (2007) 284–293, <https://doi.org/10.1086/519262>.
- [37] E.T. Piperaki, G.A. Syrogiannopoulos, L.S. Tzouveleki, G.L. Daikos, Klebsiella pneumoniae: virulence, biofilm and antimicrobial resistance, *Pediatr Infect Dis J* 36 (2017) 1002–1005, <https://doi.org/10.1097/INF.0000000000001675>.
- [38] K.H.P. Riwu, M.H. Effendi, F.A. Rantam, A.R. Khairullah, A. Widodo, A review: Virulence factors of Klebsiella pneumoniae as emerging infection on the food chain, *Vet World* 15 (2022) 2172–2179, <https://doi.org/10.14202/vetworld.2022.2172-2179>.
- [39] N. Gohil, R. Ramírez-García, H. Panchasara, S. Patel, G. Bhattacharjee, V. Singh, Book review: quorum sensing vs. quorum quenching: a battle with no end in sight, *Front Cell Infect Microbiol* 8 106 (2018), <https://doi.org/10.3389/fcimb.2018.00106>.
- [40] C.A. Fux, J.W. Costerton, P.S. Stewart, P. Stoodley, Survival strategies of infectious biofilms, *Trends Microbiol* 13 (2005) 34–40, <https://doi.org/10.1016/j.tim.2004.11.010>.
- [41] K. Stojowska-Swedrzyńska, D. Kuczynska-Wisnik, E. Laskowska, New strategies to kill metabolically-dormant cells directly bypassing the need for active cellular processes, *Antibiotics (basel)* 12 (2023), <https://doi.org/10.3390/antibiotics12061044>.
- [42] M.E.S. Guerra, G. Destro, B. Vieira, A.S. Lima, L.F.C. Ferraz, A.P. Hakansson, M. Darrieux, T.R. Converso, Klebsiella pneumoniae biofilms and their role in disease pathogenesis, *Front Cell Infect Microbiol* 12 (2022) 877995, <https://doi.org/10.3389/fcimb.2022.877995>.
- [43] Y.H. Ku, Y.C. Chuang, C.C. Chen, M.F. Lee, Y.C. Yang, H.J. Tang, W.L. Yu, Klebsiella pneumoniae isolates from meningitis: epidemiology, Virulence and Antibiotic Resistance, *Sci Rep* 7 (2017) 6634, <https://doi.org/10.1038/s41598-017-06878-6>.
- [44] D. Li, X. Huang, H. Rao, H. Yu, S. Long, Y. Li, J. Zhang, Klebsiella pneumoniae bacteremia mortality: a systematic review and meta-analysis, *Front Cell Infect Microbiol* 13 (2023) 1157010, <https://doi.org/10.3389/fcimb.2023.1157010>.
- [45] S. Li, S. Yu, M. Peng, J. Qin, C. Xu, J. Qian, M. He, P. Zhou, Clinical features and development of Sepsis in Klebsiella pneumoniae infected liver abscess patients: a retrospective analysis of 135 cases, *BMC Infect Dis* 21 (2021) 597, <https://doi.org/10.1186/s12879-021-06325-y>.
- [46] C. Liu, J. Guo, Characteristics of ventilator-associated pneumonia due to hypervirulent Klebsiella pneumoniae genotype in genetic background for the elderly in two tertiary hospitals in China, *Antimicrob Resist Infect Control* 7 (2018) 95, <https://doi.org/10.1186/s13756-018-0371-8>.
- [47] MarketsAndMarkets, Infectious Disease Diagnostics Market, 2022. <https://www.marketsandmarkets.com/Market-Reports/infectious-disease-diagnostics-market-116764589.html>. (Accessed 27.10.2023).
- [48] M. Eisenstein, Seven technologies to watch in 2022, *Nature* 601 (2022) 658–661, <https://doi.org/10.1038/d41586-022-00163-x>.
- [49] Y.C. Lai, H.L. Peng, H.Y. Chang, RmpA2, an activator of capsule biosynthesis in Klebsiella pneumoniae CG43, regulates K2 cps gene expression at the transcriptional level, *J Bacteriol* 185 (2003) 788–800, <https://doi.org/10.1128/JB.185.3.788-800.2003>.
- [50] W.L. Yu, M.F. Lee, M.C. Chang, Y.C. Chuang, Intrapersonal mutation of rmpA and rmpA2: A reason for negative hypermucoviscosity phenotype and low virulence of rmpA-positive Klebsiella pneumoniae isolates, *J Glob Antimicrob Resist* 3 (2015) 137–141, <https://doi.org/10.1016/j.jgar.2015.03.008>.
- [51] Y. Huang, J. Li, D. Gu, Y. Fang, E.W. Chan, S. Chen, R. Zhang, Rapid Detection of K1 Hypervirulent Klebsiella pneumoniae by MALDI-TOF MS, *Front Microbiol* 6 (2015) 1435, <https://doi.org/10.3389/fmicb.2015.01435>.
- [52] S. Ahmed Hasan, T. Fakhraddin Raheem, H. Mohammed Abdulla, Phenotypic, antibiotyping, and molecular detection of klebsiella pneumoniae isolates from clinical specimens in kirkuk, Iraq, *Arch Razi Inst* 76 (2021) 1061–1067, <https://doi.org/10.22092/ari.2021.355770.1721>.
- [53] Y. Chander, M. Ramakrishnan, N. Jindal, K. Hanson, S.M. Goyal, Differentiation of Klebsiella pneumoniae and K. oxytoca by multiplex polymerase chain reaction, *Int J Appl Res Vet Med* 9 (2011) 138.
- [54] Q. Mapipa, T.O. Digban, U.U. Nwodo, Antibiogram and detection of virulence genes among Klebsiella pneumoniae isolates from rustic hospital drains, *Gene Rep* 26 (2022) 101440, <https://doi.org/10.1016/j.genrep.2021.101440>.
- [55] H. Gao, Z. Shang, S.Y. Chan, D. Ma, Recent advances in the use of the CRISPR-Cas system for the detection of infectious pathogens, *J Zhejiang Univ Sci B* 23 (2022) 881–898, <https://doi.org/10.1631/jzus.B2200068>.
- [56] O. Piepenburg, C.H. Williams, D.L. Stemple, N.A. Armes, DNA detection using recombination proteins, *PLoS Biol* 4 (2006) e204.
- [57] N. Sharma, S. Hoshika, D. Hutter, K.M. Bradley, S.A. Benner, Recombinase-based isothermal amplification of nucleic acids with self-avoiding molecular recognition systems (SAMRS), *ChemBiochem* 15 (2014) 2268–2274, <https://doi.org/10.1002/cbic.201402250>.
- [58] A.V. Ivanov, I.V. Safenkova, A.V. Zherdev, B.B. Dzantiev, Recombinase polymerase amplification assay with and without nuclease-dependent-labeled oligonucleotide probe, *Int J Mol Sci* 22 (2021), <https://doi.org/10.3390/ijms222111885>.
- [59] A. Rani, V.B. Ravindran, A. Surapaneni, E. Shahsavari, N. Haleyr, N. Mantri, A. S. Ball, Evaluation and comparison of recombinase polymerase amplification coupled with lateral-flow bioassay for Escherichia coli O157:H7 detection using diiferent genes, *Sci Rep* 11 (2021) 1881, <https://doi.org/10.1038/s41598-021-81312-6>.
- [60] N. Li, L. Wang, F. Wang, H. Chen, S. Tao, Q. Zhu, L. Liu, W. Liang, F. Ma, Rapid detection of klebsiella pneumoniae carrying virulence gene rmpa2 by recombinase polymerase amplification combined with lateral flow strips, *Front Cell Infect Microbiol* 12 (2022) 877649, <https://doi.org/10.3389/fcimb.2022.877649>.
- [61] J. Zhou, L. Yin, Y. Dong, L. Peng, G. Liu, S. Man, L. Ma, CRISPR-Cas13a based bacterial detection platform: Sensing pathogen Staphylococcus aureus in food samples, *Anal Chim Acta* 1127 (2020) 225–233, <https://doi.org/10.1016/j.aca.2020.06.041>.
- [62] J.S. Chen, E. Ma, L.B. Harrington, M. Da Costa, X. Tian, J.M. Palefsky, J.A. Doudna, CRISPR-Cas12a target binding unleashes indiscriminate single-stranded DNase activity, *Science* 360 (2018) 436–439, <https://doi.org/10.1126/science.aar6245>.
- [63] J.S. Gootenberg, O.O. Abudayyeh, M.J. Kellner, J. Joung, J.J. Collins, F. Zhang, Multiplexed and portable nucleic acid detection platform with Cas13, Cas12a, and Csm6, *Science* 360 (2018) 439–444, <https://doi.org/10.1126/science.aag0179>.